Analysis of Low-Frequency Radio Array Mapping of D-Region Electron Densities and HF Absorption

Matthew Strong

Low Frequency Radio Group

Georgia Institute of Technology

Atlanta, GA.

matthewstrong@gatech.edu

Morris Cohen
School of Electrical and Computer Engineering
Georgia Institute of Technology
Atlanta, GA.
mcohen@gatech.edu

Abstract—We present results from an array of low-frequency (500 Hz - 500 kHz) radio receivers, passively recording VLF (3-30 kHz) emissions from natural lightning and navy VLF transmitters. A series of signal processing, machine learning, and tomographic techniques amalgamates this dataset to reconstruct the 3D D-region (60-90 km) ionospheric electron density profiles over the Gulf of Mexico and Southeastern USA. We present profiles over a selected 13-day period in August 2017 during which time there was a solar eclipse and multiple major solar flares. The VLF electron density profiles are also used to infer HF absorption as a function of location and time, a technique described in this paper. We use this to validate our D-region inferences by comparing against a ground-based ionosonde instrument

Index Terms—VLF Array, Ionosonde, D-Region, Ionosphere

I. Introduction

The lowest and most dynamic region of the ionosphere is the D-region (60 - 90 km) which is too high for balloons, too low for satellites, and too sparsely charged for radars [1]. Nonetheless, this ionosphere layer impacts trans-ionospheric and over-the-horizon navigation and communication signals [2]. The D-Region is also used in measuring a host of geophysical phenomena, including solar flares, acoustic gravity waves, electron precipitation, among others [3]–[5].

The High Frequency (HF, 3-30 MHz) band is commonly used for ionospheric sensing and for long-range communications such as shortwave broadcasting and transoceanic aviation communications [6], [7]. Because HF frequencies are significantly attenuated by the D-Region, however, a strongly ionizing solar event drastically increasing D-Region electron density may render HF propagation infeasible.

Very Low Frequency and Low Frequency (VLF/LF, 3-300 kHz) signals propagate efficiently to global distances in a waveguide formed by the ground and the D-Region, and reflect from the D-region itself. Signal fidelity typically increases with stronger D-Region electron density, such as from a solar flare, thereby making VLF more resilient in instances when HF signals are weaker. VLF signals, however, are difficult to generate because of long wavelengths (10 km at 30 kHz) and have therefore been mostly restricted in terms of applications to submarine communications [8] and an early global navigation system [9].

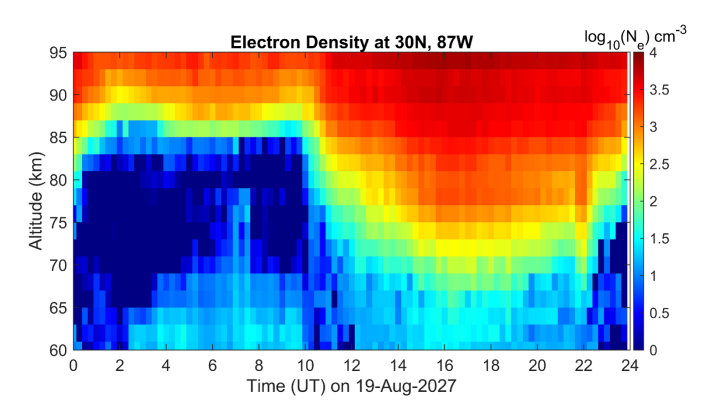


Fig. 1: Tomography at Eglin, Florida, on August 19, 2017

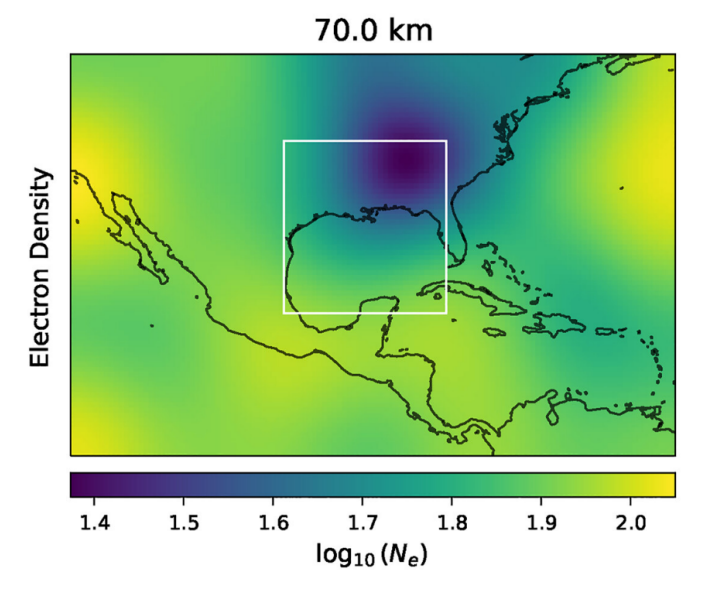


Fig. 2: D-Region electron density of August 21 solar eclipse at 70 km, 18:30 UT. From Richardson, [10]

VLF remote sensing is, nonetheless, useful to characterize the D-Region. A recently-developed set of algorithms [10]–[14] utilizes an array of VLF receivers detecting two signals of interest: (1) VLF transmitters, which are operated by the Navy for communications, and (2) sferics, or wide-band impulsive emissions from lightning strokes, both of which propagate from global distances to the receiver. By processing and aggregating sferics and VLF transmitter signals, we construct, via machine learning, a tomography of the D-Region electron density.

In this study, data is analyzed from August 19 to 31, 2017, during which time multiple solar flares and a total solar eclipse across the southern United States occurred.

The receiver consists of two orthogonal, air-core, wire-loop antennas, sensitive to the 500 Hz - 500 kHz band, with \sim 20 ns timing accuracy, and few fT/rt-Hz sensitivity [15].

II. McCormick-Gross-Richardson Model

The VLF transmitters are first processed by demodulating the Minimum Shift Keying (MSK) modulation signal, yielding the amplitude, carrier phase, and clock phase. These outputs, on two orthogonal loop antennas, allow reconstruction of the polarization ellipse [16] even with the 90-degree ambiguity inherent in MSK. The amplitude and phase of the extracted VLF signal is then fed into a pre-trained artificial neural network (ANN) [11], yielding an estimate of two parameters of the electron density, for each transmitter-to-receiver path [17].

Next, the sferics are processed. In this stage, the MSK transmitter signals previously calculated are removed. Events from a lightning location detection system such as GLD360 [18], [19] are then matched with sferics in the VLF data. Sferics from the same storm and close in time are clustered and precisely time-aligned to account for variability in lightning current and the error of the lightning location [12]. This timealigned sferic carries the average characteristic information about the ionosphsere along the path from the thunderstorm location to the receiver. This information is then matched to a preexisting table of calculated sferics, for each storm-toreceiver path, for a set of four-parameter, D-Region profile models [13]. The best-fit profile is then selected. Using a neural network, an electron density tomography is then built by aggregating the many path-averaged D-Region profiles along the storm-receiver paths [10]. Finally the results of the VLF transmitters and VLF sferic analyses are unified, and a final tomographic reconstruction is produced [14].

With roughly forty lightning strikes occurring every second [20] and the additional active VLF transmitters transmitting during the time of this study, there are enough source-to-receiver paths every five minutes to build a high-resolution profile of electron density across the continent [21], [22].

Two depictions of this tomography are shown in Figure 1 and Figure 2. Figure 1 shows this tomography near Eglin, Florida (30° N, 87° W) across altitude and time. Figure 2 shows this tomography at an altitude of 70 km and at 18:30 UT across North America.

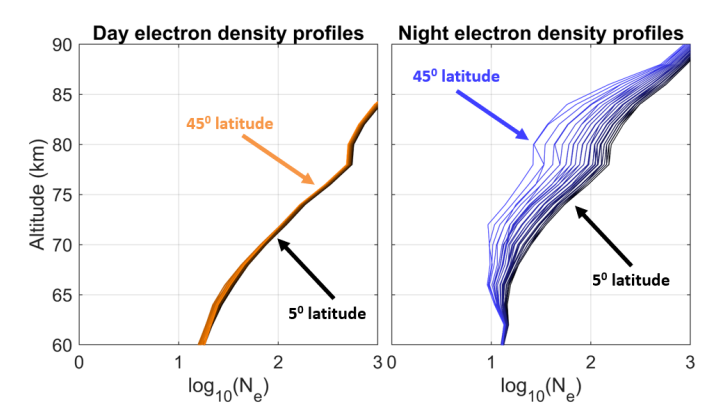


Fig. 3: Initial Climatology Results for the D-Region

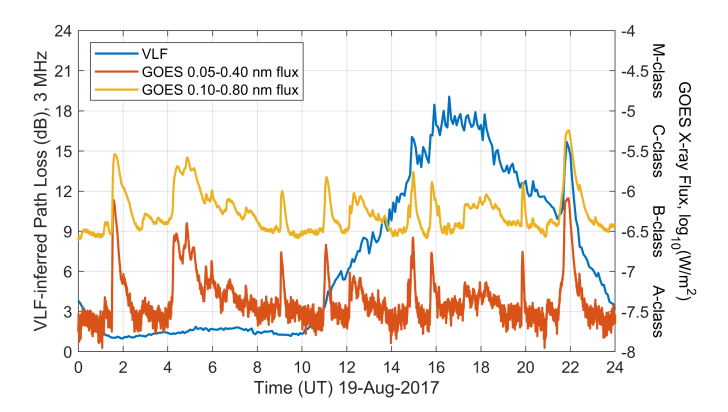


Fig. 4: VLF inferred absorption (O-Mode) and X-Ray flux plotted for August 19, 2017

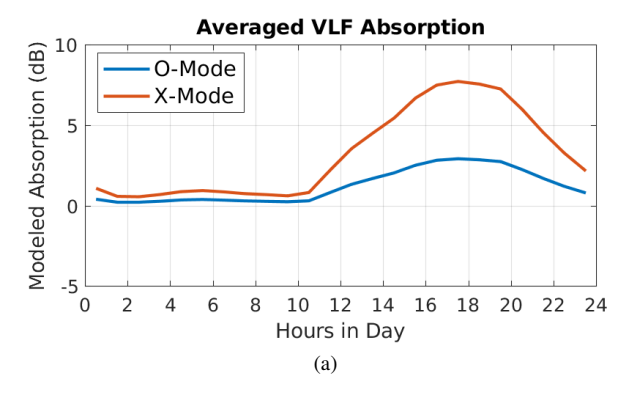
III. D-REGION CLIMATOLOGY

Figure 3 shows initial efforts to build a D-region climatology with the results. For each 5-minute block of time, we average the electron density profile across all longitudes, and then average all the profiles for either daytime (left panel) or nighttime (right panel). The figure shows the electron density profile as a function of latitude, between 5° N and 45° N. During the daytime, the electron density profile changes by a very small amount only. During the northern hemisphere summer months, the sun is nearly overhead over much of these latitudes, hence the zenith angle variation is relatively small. If repeated in the wintertime, there will be a larger difference between low and mid latitudes on the northern hemisphere.

However, at nighttime, a more significant dependence on latitude appears, with mid latitudes being lower in electron density by about half an order of magnitude compared to low latitudes.

IV. VALIDATION WITH HF

Obtaining validation data is difficult due to the lack of independent and direct measurements of the D-region. We present two methods to validate our D-Region electron density estimates. Our D-region estimates allow us to calculate/infer the HF absorption, by calculating the Appleton-Hartree index



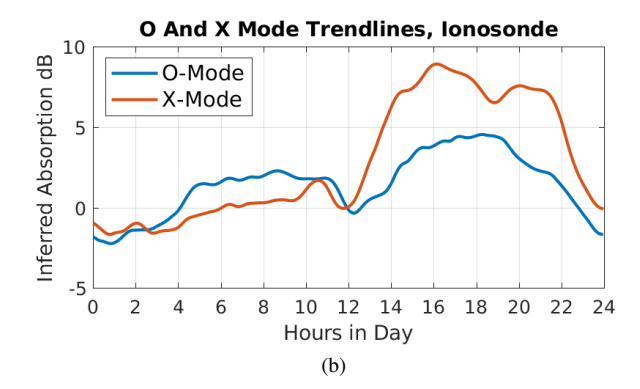


Fig. 5: A comparison of VLF and ionosonde inferred absorption; a days worth of averaged absorption values from August 19 to 31, 2017

of refraction, and integrating the HF absorption through the D-region. Since this is more readily observable, and correlated with respect to solar x-ray flux, we use this method for validation.

A. Solar Flare HF Absorption

Figure 4 displays GOES X-ray Flux in two different bands, which show an X-class solar flare at 22 UT on August 19, 2017. This large solar flare clearly corresponds with an increase in VLF-inferred HF absorption.

As observed throughout the daytime, and especially at 22 UT, there exists a strong correlation between X-Ray flux and observed D-Region absorption caused by an increase in ionization.

B. Correlation with an Ionosonde

Ionosondes are radars, typically used to interrogate the E and F regions by measuring the characteristic reflection ranges of a wideband signal from 1 to 10 MHz [23]. The ionsonde works by transmitting (and receiving) an Ordinary-Mode (O-Mode, LHCP) and Extraordinary-Mode (X-Mode, RHCP) polarized wave along zenith from a collocated ground transmitter and receiver.

The ionosonde also records the amplitude for each polarization, and 0.025 MHz-discretized frequency within the band. But this information is rarely used. Free-space loss accounts for a reduced signal strength by a factor of $1/r^2$ in addition to variable absorption in the D-Region. We multiply each received amplitude by r^2 , thereby adjusting for free-space loss and isolating absorption from the D-region, or other factors like focusing and irregularity scattering. We apply this technique to both single-hop and double-hop signals.

The inferred D-Region absorption from both the ionosonde data and VLF is averaged over a twelve day period from August 19 to 31, 2017 and an interpolated average spline is fit for both of the modes and is shown in Figure 5. A simple comparison reveals a strong correlation between the two disparate methods of D-Region absorption inference suggesting an accurate electron density model.

V. CONCLUSION

The McCormick-Gross-Richardson VLF tomography model make use of a global VLF array network which harvests pertinent D-Region information from VLF transmitters and lightning-based sferics around the world. The accuracy of this model is revealed through an observation of natural phenomenon within VLF inferred absorption, an investigation of D-Region climatology, and correlation between VLF inferred and ionosonde inferred D-Region absorption. Such a verification supports the installation of more VLF array receivers, of which receiver installments north into the Arctic and south into the Caribbean are pending. A more robust data-set of the D-Region will provide a foundation for VLF communication and positioning technologies while also allow users of HF technologies to infer absorption in the D-Region in the event of a high ionoization event such as a geomagnetic storm.

ACKNOWLEDGMENT

This work was supported by the National Science Foundation under grants AGS-2221765404 and AGS-2139916 to the Georgia Institute of Technology, by the Office of Naval Research under Award N000142312111 to the Georgia Institute of Technology, and by the Air Force Office of Scientific Research under Award FA9550-23-1-0164 to the Georgia Institute of Technology.

REFERENCES

- Michael C. Kelley. *D-Region Fundamentals*, chapter 1.3. Academic Press, 2009.
- [2] S.L. Bernstein, M.L. Burrows, J.E. Evans, A.S. Griffiths, D.A. McNeill, C.W. Niessen, I. Richer, D.P. White, and D.K. Willim. Long-range communications at extremely low frequencies. *Proceedings of the IEEE*, 62(3):292–312, 1974.
- [3] Neil R Thomson, Craig J Rodger, and Mark A Clilverd. Large solar flares and their ionospheric d region enhancements. *Journal of Geophysical Research: Space Physics*, 110(A6), 2005.
- [4] Gordana Jovanovic. Acoustic–gravity waves and their role in ionosphere–lower thermosphere coupling. Annales Geophysicae Discussions, 2024:1–17, 2024.
- [5] Sean J Lev-Tov, Umran S Inan, and Timothy F Bell. Altitude profiles of localized d region density disturbances produced in lightning-induced electron precipitation events. *Journal of Geophysical Research: Space Physics*, 100(A11):21375–21383, 1995.

- [6] E. M. Warrington, N. C. Rogers, A. J. Stocker, D. R. Siddle, H. A. H. Al-Behadili, F. Honary, M. J. Beharrell, D. H. Boteler, D. W. Danskin, and N. Y. Zaalov. Developments in hf propagation predictions to support communications with aircraft on trans-polar routes. In 2017 Progress In Electromagnetics Research Symposium Spring (PIERS), pages 1953–1959, 2017.
- [7] James M Headrick, Stuart J Anderson, and Merrill Skolnik. Hf overthe-horizon radar. *Radar handbook*, 20, 2008.
- [8] AD Watt. Vlf radio engineering. 1967.
- [9] E.R. Swanson. Omega. Proceedings of the IEEE, 71(10):1140–1155, 1983.
- [10] David K Richardson, Jackson C McCormick, and Morris B Cohen. Ad-region ionospheric imaging method using sferic-based tomography. *Journal of Geophysical Research: Space Physics*, 128(8):e2023JA031573, 2023.
- [11] NC Gross and MB Cohen. Vlf remote sensing of the d region ionosphere using neural networks. *Journal of Geophysical Research: Space Physics*, 125(1):e2019JA027135, 2020.
- [12] Jackson C McCormick, Morris B Cohen, NC Gross, and RK Said. Spatial and temporal ionospheric monitoring using broadband sferic measurements. *Journal of Geophysical Research: Space Physics*, 123(4):3111–3130, 2018.
- [13] JC McCormick and MB Cohen. A new four-parameter d-region ionospheric model: Inferences from lightning-emitted vlf signals. *Journal of Geophysical Research: Space Physics*, 126(12):e2021JA029849, 2021.
- [14] David K Richardson and Morris B Cohen. Unifying vlf transmitter and sferic modeling efforts via tomography. *Journal of Geophysical Research: Space Physics*, 128(11):e2023JA031989, 2023.
- [15] Morris B. Cohen, Ryan K. Said, Evans W. Paschal, Jackson C. Mc-Cormick, Nicholas C. Gross, Lee Thompson, Marc Higginson-Rollins, Umran S. Inan, and Jeffrey Chang. Broadband longwave radio remote sensing instrumentation. *Review of Scientific Instruments*, 89(9):094501, 09 2018.
- [16] NC Gross, MB Cohen, RK Said, and M Gołkowski. Polarization of narrowband vlf transmitter signals as an ionospheric diagnostic. *Journal* of Geophysical Research: Space Physics, 123(1):901–917, 2018.
- [17] David K Richardson and Morris B Cohen. Seasonal variation of the d-region ionosphere: Very low frequency (vlf) and machine learning models. *Journal of Geophysical Research: Space Physics*, 126(9):e2021JA029689, 2021.
- [18] R. K. Said, U. S. Inan, and K. L. Cummins. Long-range lightning geolocation using a vlf radio atmospheric waveform bank. *Journal of Geophysical Research: Atmospheres*, 115(D23), 2010.
- [19] R. K. Said, M. B. Cohen, and U. S. Inan. Highly intense lightning over the oceans: Estimated peak currents from global gld360 observations. *Journal of Geophysical Research: Atmospheres*, 118(13):6905–6915, 2013.
- [20] Hugh J Christian, Richard J Blakeslee, Dennis J Boccippio, William L Boeck, Dennis E Buechler, Kevin T Driscoll, Steven J Goodman, John M Hall, William J Koshak, Douglas M Mach, et al. Global frequency and distribution of lightning as observed from space by the optical transient detector. *Journal of Geophysical Research: Atmospheres*, 108(D1):ACL-4 2003
- [21] MB Cohen, NC Gross, MA Higginson-Rollins, RA Marshall, M Gołkowski, W Liles, D Rodriguez, and J Rockway. The lower ionospheric vlf/lf response to the 2017 great american solar eclipse observed across the continent. *Geophysical Research Letters*, 45(8):3348–3355, 2018
- [22] Morris B Cohen, Umran S Inan, and Evans W Paschal. Sensitive broadband elf/vlf radio reception with the awesome instrument. *IEEE Transactions on Geoscience and Remote Sensing*, 48(1):3–17, 2009.
- [23] Bodo W Reinisch, Ivan A Galkin, GM Khmyrov, AV Kozlov, K Bibl, IA Lisysyan, GP Cheney, X Huang, DF Kitrosser, VV Paznukhov, et al. New digisonde for research and monitoring applications. *Radio Science*, 44(01):1–15, 2009.